



HAL
open science

The IERS EOP 14C04 solution for Earth orientation parameters consistent with ITRF 2014

Christian Bizouard, Sébastien Lambert, César Gattano, Olivier Becker,
Jean-Yves Richard

► **To cite this version:**

Christian Bizouard, Sébastien Lambert, César Gattano, Olivier Becker, Jean-Yves Richard. The IERS EOP 14C04 solution for Earth orientation parameters consistent with ITRF 2014. *Journal of Geodesy*, 2019, 93 (5), pp.621-633. 10.1007/s00190-018-1186-3 . hal-02302240

HAL Id: hal-02302240

<https://hal.science/hal-02302240>

Submitted on 30 Apr 2024

HAL is a multi-disciplinary open access archive for the deposit and dissemination of scientific research documents, whether they are published or not. The documents may come from teaching and research institutions in France or abroad, or from public or private research centers.

L'archive ouverte pluridisciplinaire **HAL**, est destinée au dépôt et à la diffusion de documents scientifiques de niveau recherche, publiés ou non, émanant des établissements d'enseignement et de recherche français ou étrangers, des laboratoires publics ou privés.

The IERS EOP 14C04 solution for Earth orientation parameters consistent with ITRF 2014

Christian Bizouard¹ · Sébastien Lambert¹ · César Gattano² · Olivier Becker¹ · Jean-Yves Richard¹

Abstract

The Earth Orientation Center of the International Earth Rotation and Reference Systems Service (IERS) has the task to provide the scientific community with the international reference time series of Earth orientation parameters (EOP), referred to as IERS EOP C04 or C04. These series result from a combination of operational EOP series derived from VLBI, GNSS, SLR, and DORIS. The C04 series were updated to provide EOP series consistent with the set of station coordinates of the ITRF 2014. The new C04, referred to as IERS EOP 14C04, is aligned onto the most recent versions of the conventional reference frames (ITRF 2014 and ICRF2). Additionally, the combination algorithm was revised to include an improved weighting of the intra-technique solutions. Over the period 2010–2015, differences to the IVS combination exhibit standard deviations of $40\ \mu\text{s}$ for nutation and $10\ \mu\text{s}$ for UT1. Differences to the IGS combination reveal a standard deviation of $30\ \mu\text{s}$ for polar motion. The IERS EOP 14C04 was adopted by the IERS directing board as the IERS reference series by February 1, 2017.

Keywords Earth rotation · Space and geodetic techniques · Combination

1 Introduction

The Earth rotation is not uniform. It fluctuates under the influence of the surrounding celestial bodies, the hydro-atmospheric circulation, and fluid core—mantle interaction. The interaction of the Sun and the Moon with the Earth’s equatorial bulge produces the precession–nutation, modeled to a very good accuracy (Mathews et al. 2002; Capitaine et al. 2003). Residuals to very long baseline interferometry (VLBI) observations—of 0.2 millisecond of arc (mas) in rms—include a number of non-modeled effects (Dehant et al. 2003) dominated by the free core nutation, whose excitation mechanisms remain unclear (Chao and Hsieh 2015) and thereby unpredictable. Polar motion, namely the rotation pole displacement relatively to the crust, is strongly connected to air–water mass transport at hourly to decadal time scales (Barnes et al. 1983; Ponte et al. 1998; Chen et al. 2013) but remains poorly predictable (e.g., Kalarus et al. 2010) on the basis of the current hydro-atmospheric global circulation

models. Earth’s rotation velocity also varies significantly, causing the length-of-day (LOD) changes or variations of the Earth rotation time UT1 with respect the atomic time TAI or UTC. Significant contribution to UT1 or LOD arise from zonal tides and are modeled with a precision of $\sim 5\ \mu\text{s}$ on UT1, smaller than the observational uncertainty (Defraigne and Smits 1999; Ray and Erofeeva 2014). Nevertheless the largest part of the fluctuations in UT1 and LOD comes from geophysical processes, especially mass transport within the atmosphere and the fluid core. The latter is considered as responsible for multi-decadal LOD variations of several milliseconds (ms) (Hide et al. 2000) and nearly 5.9-year oscillation of weaker amplitude (Holme and Viron 2013). These are superimposed to the slight secular braking (1.6 ms/cy) due to the dissipation in the Earth–Moon system (Yoder et al. 1983). The atmosphere drives the LOD at seasonal and sub-seasonal scales (Rosen and Salstein 1983; Chao and Yan 2010) and even produces major interannual oscillations, among them El Niño events (e.g., Chao 1984).

The irregularities of these variations are parametrized through the so-called Earth orientation parameters (EOP), composed of corrections dX and dY to the conventional precession–nutation model, pole coordinates x and y , and the difference UT1–UTC. To EOP, we append their time derivatives (or apart from a factor for UT1), like LOD and polar

✉ Christian Bizouard
christian.bizouard@obspm.fr

¹ Observatoire de Paris / SYRTE, Groupe universitaire PSL, CNRS, Universités de la Sorbonne, Paris, France

² Laboratoire d’Astrophysique de Bordeaux, Paris, France

coordinates rates. In light of the present technical capabilities, these EOP are routinely derived at time rate of 1 day for pole coordinates, and 1–7 day for UT1 and nutation offsets. Pole coordinates as well as UT1 also contain diurnal and sub-diurnal signal, mainly resulting from ocean tides and up to 1 mas or $100\ \mu\text{s}$. In respect of their regularity, these tidal high-frequency oscillations are not monitored permanently. By adding their conventional model to x , y and UT1, the five EOP parameters fully determine the transformation between a terrestrial reference frame (TRF) and a celestial reference frame (CRF) (see, e.g., Petit and Luzum 2010) and are more generally needed for real-time orbit determination, positioning, and interplanetary navigation. The consistent reduction of geodetic observations requires the use of International TRF (ITRF) and International CRF (ICRF). Here, the C04 data are dedicated to provide reference EOP consistent with ITRF and ICRF at a daily time rate. Subsequently C04 do not include daily and sub-daily terms up to 0.5 mas, mostly caused by ocean tides. This ocean tidal effect can be modeled by a sum of diurnal and semi-diurnal harmonic waves and is the object of an IERS conventional model (Petit and Luzum 2010).

To achieve the global geodetic observing system (GGOS) recommendation of an accuracy of 1 mm in position of station coordinates of the ITRF at weekly time scale (Plag et al. 2009), EOP must be known at better than 0.03 mas. Since predictive models are insufficient to reach such an accuracy, EOP have to be derived observationally from space and geodetic techniques: VLBI, laser ranging to dedicated artificial satellites (SLR), global navigation satellite system (GNSS), and Doppler orbitography by radiopositioning integrated on satellite (DORIS). However, none of the technique provides the full set of EOP except VLBI. Moreover, EOP are derived according to different strategies pertaining to algorithm, models, or station networks. For instance, GNSS only provides pole coordinates and LOD; VLBI provides all EOP, but the associated pole coordinates are not as sampled as the GNSS ones. For these reasons, a combination of the results from different techniques appears as an optimal way to build up EOP series that keep intact the strengths of each technique, and mitigate their weaknesses. The International Earth Rotation and Reference Systems Service (IERS) has entrusted to the Earth Orientation Center (EOC) component, hosted by Paris Observatory, with the task of combining operational EOP series for providing the international reference referred to as IERS EOP C04 (abbreviated in C04).

Until the release of the International Terrestrial Reference Frame (ITRF) 2014 (Altamimi et al. 2016), the C04 was referred to the ITRF 2008 (Altamimi et al. 2011) and to the second realization of the International Celestial Reference Frame (ICRF2) (Fey et al. 2015). This ancient version of the C04 will be referred to as 08C04 in the following (Bizouard and Gambis 2009). Comparisons between 08C04

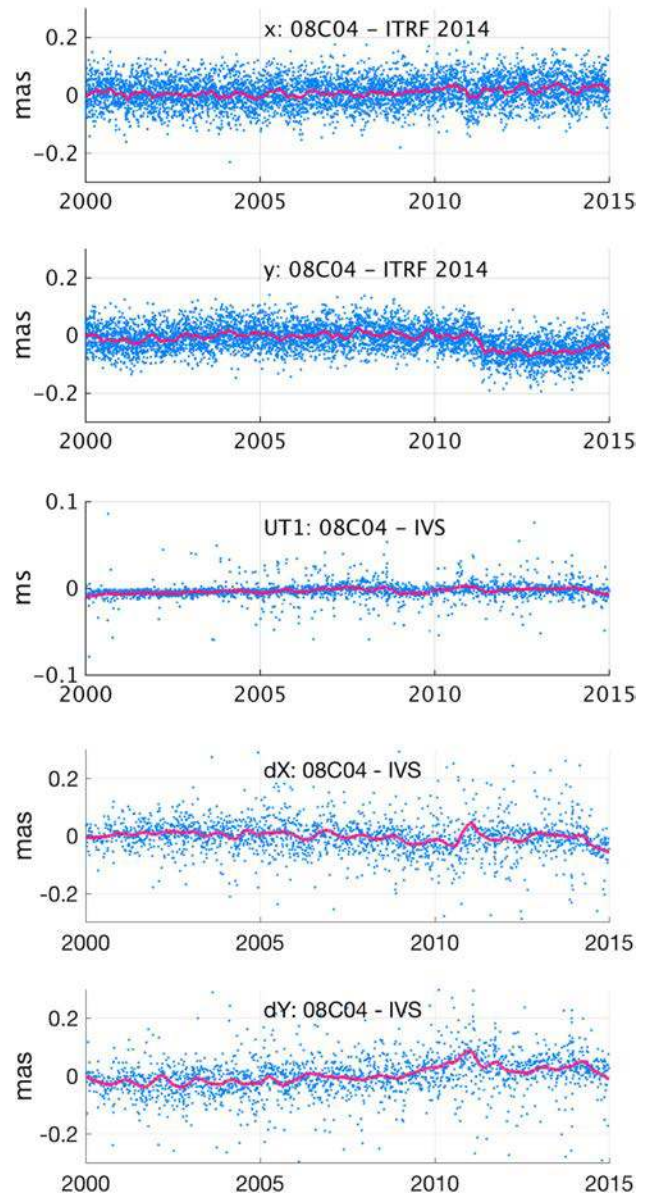


Fig. 1 Differences in (top) pole coordinates between 08C04 and ITRF 2014, and (bottom) UT1/nutation offsets between 08C04 and IVS. The thick, red curve represents a 3-month smoothing

and the EOP series produced jointly with the ITRF 2014 solution revealed bias of up to $50\ \mu\text{as}$ in y pole coordinate (see Fig. 1, top part), just above the corresponding mean formal uncertainty estimated by IGS. This bias reflects some change in handling the terrestrial system by IGS, probably mixed with a wrong network correction applied to IGS time series, not updated since 2010. This demonstrated the relevance of reprocessing the C04 to make it consistent with the new ITRF. [For more insights into the sensitivity of EOP to reference frames, see also (Belda et al. 2017).] This paper describes this reprocessing.

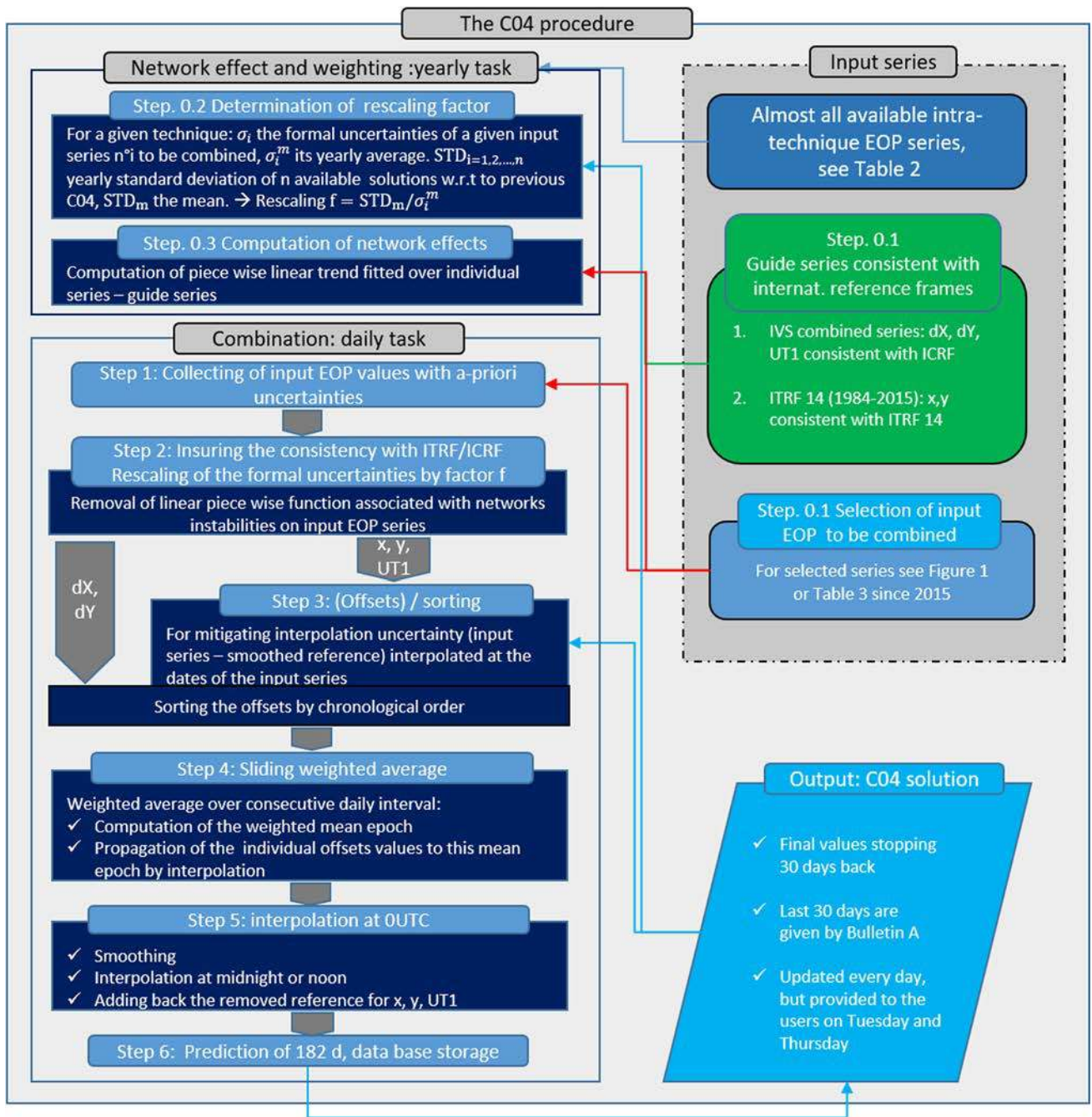


Fig. 2 Schematic of the C04 combination

2 Data preparation

The C04 algorithm is split in two parts, in which the schematic is displayed in Fig. 2. The initial part is the data preparation, done once a year only, to be distinguished from the combination procedure itself—the second part—which is done on a daily basis. Data preparation is composed of the selection of input EOP series (step 0.1), the rescaling of the formal uncertainties provided with EOP values (step 0.2),

and the characterization of their eventual inconsistency with respect to space reference frame (step 0.3), as described in more details now.

Step 0.1: Selection of a set of N EOP series for successive yearly intervals. Each civil year, for a given EOP (UT1-UTC, LOD) or a set of EOP ($x/y, dX/dY$), we select or we update a set of operational or final EOP series derived from the four techniques. The EOP value are called “final” when they are

Table 1 EOP series entering the intra-technique calibration of uncertainties from 1984 onward

	x, y	UT1	dX, dY	LOD	Period
VLBI AUS	×	×	×		1983–2017
VLBI BKG	×	×	×		1984–2017
VLBI GSFC	×	×	×		1979–2017
VLBI IAA	×	×	×		1984–2017
VLBI IVS F	×	×	×		1984–2017
VLBI OPA	×	×	×		1979–2017
VLBI USNO	×	×	×		1979–
VLBI BKG intensive		×			1999–
VLBI GSFC intensive		×			1991–
VLBI IAA intensive		×			1986–
VLBI OPA intensive		×			2006–
VLBI USNO intensive		×			2000–
VLBI PUL intensive		×			1999–
VLBI GSI intensive		×			2003–
GNSS CODE	×			×	1997–
GNSS EMR	×			×	1996–
GNSS JPL	×			×	1996–
GNSS GFZ	×			×	1998–
GNSS ESOC	×			×	1996–
GNSS IGS final	×			×	2001–
GNSS NGS	×			×	2002–
GNSS MIT	×				2012–
GNSS SIO	×			×	1996–
SLR CGS	×			×	2002–
SLR CSR	×				1976–1998
SLR IAA	×			×	1992–2009
SLR ILRS	×			×	1998–
SLR MAO	×				1983–2001
SLR OCA	×				1993–2007
SLR PUL	×			×	2003–2012
DORIS IDS	×			×	2015–
DORIS INASAN	×			×	2015–

Some of them enter also the C04 combination. These series can be downloaded from <http://iers.obspm.fr/eop-pc/index.php?index=analysis&lang=en/>

determined once for all, while younger values (between about 30 days into the past and the current epoch) are referred to as “rapid” or operational and they can undergo change in the next treatments.

The available series since 1984, as stored in our data base, are listed in Table 1. The series used in the C04 combination from 1984 are shown in Fig. 3. From 2015, we consider the combined series provided by the IGS, IVS, and ILRS. But, from 1993 to 2015, pole coordinates are exclusively based upon the multi-technique solution produced jointly with the ITRF 2014. Since the rapid IVS combination does not process the full geodetic VLBI observational data base, excluding some sessions not specifically designed for EOP monitoring, we also consider “individual” solutions from several analysis centers susceptible to provide intermediate estimates of

UT1-UTC and nutation offsets (see Sect. 4). As the present ILRS combined solution does not cover dates prior to 1999, SLR contribution to pole coordinates is represented by the solution of Center of Space Research (CSR). The inclusion of satellite LOD series begins in 1997 with the solution of Bern University (CODE). Before 1997, LOD is derived from UT1 values according to

$$\text{LOD} = -D \frac{d(\text{UT1} - \text{TAI})}{dt}, \quad (1)$$

where $D = 86,400$ s is the nominal length of day.

Since 2015, in respect to the increasing accuracy of DORIS pole coordinates, below $200 \mu\text{as}$, we added the combined solution of the International DORIS Service (IDS 2018).

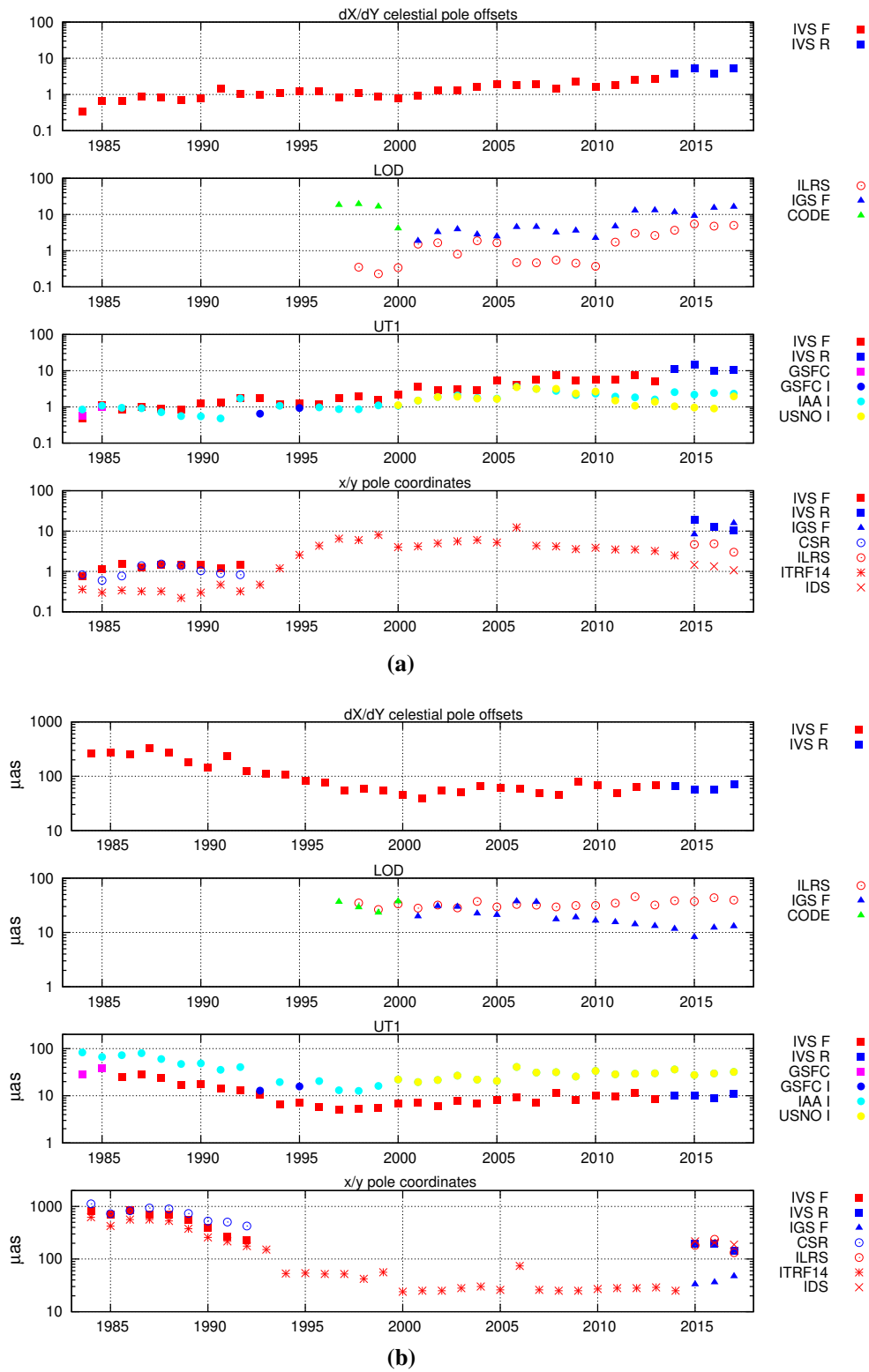


Fig. 3 Yearly set of selected series entering into the C04 combination from 1984 to 2018, and evolution of their uncertainty. Upper plot: yearly scaling factor f_j of the selected series for their combination from 1984 to 2017 (final solution). Bottom plot: the same for the intra-technique mean standard deviation STD_m (two series of the same technique have the same STD_m and are superposed) expressed in μas for celestial pole

offsets/pole coordinates and in μs for UT1/LOD. For each series, we indicate the underlying technique by a given symbol: filled square for VLBI, filled circle for VLBI I, filled triangle for GNSS, open circle for SLR, cross for DORIS, and star for intra-technique combined series. **a** Yearly calibrating factor f_j . **b** Calibrated mean uncertainty in μas (x , y/dX , dY) or in μs (UT1/LOD)

The selected EOP series entering the combination have to be made “consistent.” This is the object of the steps 0.2 and 0.3, detailed now.

Step 0.2. Rescaling of the formal uncertainties. The first inconsistency affecting EOP concerns their formal uncertainty. A question arising when comparing signals representing the same quantity but obtained through independent analyses and/or techniques is whether one can trust the standard errors. This question is of particular interest since the data weighting that will be used further for the combination is based on these standard errors. It appears that, for a given technique, standard errors associated with different EOP solutions generally do not fit the differences between solutions, suggesting underestimated errors. Interestingly, similar evidences were raised in several studies involving VLBI (Herring et al. 2002; Gipson 2007; Fey et al. 2015). These discrepancies can have several causes: (i) the analysis strategies adopted by analysts can lead to significantly different solutions without clear information on the quality of the processing; (ii) the propagation of the errors from the observable through the inversion algorithm up to the final estimated parameters might not be realistic when the measurement correlation is not accounted for Durando and Mana (2002).

We propose therefore to rescale the standard errors of the series to make them consistent with the average standard deviation of their pair differences, as follows. Over a given time interval T (1 year in the present C04 procedure), by selecting series of the same technique in Table 1, all paired differences with respect to a given reference series are built, in which the corresponding standard deviations (STD_i for series i) are computed. The mean of all those standard deviation, noted STD_m , sums up the intra-technique discrepancy for the considered EOP. On the other hand, EOP of series i is given with its formal error $\sigma_i(t)$ at date t . We compute the corresponding mean σ_i^m over the time interval T . If discrepancies between series is purely random, then STD_m is a rough estimate of the mean uncertainty, and it can be compared with the mean formal error σ_i^m . This leads to rescale the formal error $\sigma_i(t)$, becoming

$$\tilde{\sigma}_i(t) = f_i \sigma_i(t) \quad \text{with} \quad f_i = \text{STD}_m / \sigma_i^m. \quad (2)$$

However, such a method acts to privilege the similar series and discard series, which have singular behavior with respect to the others. Similarity does not insure that the corresponding EOP values are better, for it can stem from similar processing. In this respect, for a given technique, we select a set of series obtained by different software in order to mitigate such a possible bias in rescaling the formal error. The selected series are reported in Fig. 3. The same figure provides the yearly calibrating factor f_i for each EOP and series

entering the C04 combination. The striking discrepancy of f_i from one series to another (up to an order of magnitude) reflects the non-homogeneity of a priori formal uncertainties. A strong increase of f_i is notable for the ITRF 2014 pole coordinate series after 1995, probably reflecting the advent of GNSS series.

Step 0.3. Estimation of EOP series inconsistency with respect to the ICRF and ITRF. The EOP series have to be aligned onto the current realizations of the ICRF and ITRF. Being based on sub-networks of ITRF stations and, for VLBI, restricted coverage of the quasars defining the ICRF, the intra-technique series can drift in a random-like way with respect to other series referred to discrepant reference frames (Zhu and Mueller 1983; Belda et al. 2017). In the 1980s, inconsistencies were as large as 1 mas. They are now reduced to less than $100 \mu\text{as}$ for polar motion, $10 \mu\text{s}$ for UT1, and $50 \mu\text{as}$ for nutation offsets, but they are still significant regarding the accuracy of the techniques and the expected stability. To correct from these “network effects,” we model trends, defined as excursions of selected series away from the guide series on interannual to decadal time scales, by continuous piecewise linear functions. After a preliminary examination of the series, a small number of nodes were selected on the first day of 1993, 2000, 2010, and 2012. The first node corresponds to the introduction of GNSS.

Two data sets are “outstanding” in the sense that they provide EOP robustly aligned onto the conventional reference frames. These data sets are (i) the daily pole coordinate provided along with the ITRF 2014 realization over 1993–2015 (Altamimi et al. 2016), and (ii) the latest quarterly combined solution for UT1 and nutation offsets provided by International VLBI Service for geodesy and astrometry (Schuh and Behrend 2012) and spanning over 1984–2016. Both series result from weighted combinations of pre-reduced normal equations and solved with suitable minimal constraints. For the pole coordinates, input data comes from technique centers including IVS, International GNSS Service (Dow et al. 2009), International Laser Ranging Service (Pearlman et al. 2005) and International DORIS Service (Willis et al. 2010). For the second solution, data are provided by individual analysis centers of the IVS.

So, we assume here that (i) the celestial pole offsets of the IVS solution yield the direction of the CIP in the ICRF without any significant multi-decadal trend (except the variations due to the mismodeling of the precession and nutation); (ii) UT1-UTC or UT1—TAI from the IVS-combined solution yields the non-uniformly varying part of the Earth rotation angle (multiplying it by the nominal Earth rotation velocity $\Omega = 7.292\,115\,146\,706\,4 \cdot 10^{-5}$ rad/s) around the CIP without any significant drift and bias; (iii) the pole coordinates of the ITRF 2014 solution give the direction of the CIP in the ITRF without multi-decadal trend. In the following, these

series will be referred to as IVS and ITRF 2014, or guide series, since they help us to stick the combination to the ITRF 2014 and ICRF2.

Notice that the choice of ITRF 2014 EOP solution as guide series for pole coordinates is not unique, for we could have used the EOP associated with the release of DTRF 2014 (Seitz et al. 2016) (the German TRF) or the EOP of the JTRF 2014 solution, produced by JPL (Abbondanza et al. 2017), without introducing significant changes in multi-decadal drift in paired differences with IGS, ILRS, and IDS solutions.

The guide series do not span over most recent epochs (for instance, the ITRF 2014 EOP series stop in 2015), and the modeled linear trends in the differences between operational and guide series are currently extrapolated to new epochs. As the 14 C04 EOP values are not updated back in the past (except the last 30 days), any change in ICRF will not be reflected by nutation and UT1 values prior to this change.

The LOD guide series is naturally the one obtained from UT1 IVS guide series by applying (1). Instabilities in satellite orbits, mainly attributed to solar radiation pressure (Bar-Sever and Russ 1997) induce a severe and unpredictable drift in satellite-derived LOD with respect to this “UT1 consistent” LOD. Moreover, GNSS or SLR LOD series present offsets of 20 μ s at annual scale. Any variation in the differences of the GNSS/SLR LOD series with respect to LOD guide series over time scales larger than two weeks are considered as spurious (two weeks can be seen as the time scale over which GNSS becomes unstable, while the stability of VLBI is improved) and eliminated by a high-pass (Vondrák 1969) filter (cutoff period of 30 days).

3 Combination

For each series entering into the combination, yearly calibrating factor f of the formal uncertainties and piecewise linear correction are stored in the “network” files. In turn, these ones indicate for a given year the EOP series to be combined, the associated factors f for each EOP, and possible network correction under the form of bias and rate. Then, the combination can start achieving the following steps.

Step 1: Collecting of input EOP values selected in step 0.1 including their a priori uncertainties.

Step 2: Making the series homogeneous. After having read the network file of the corresponding time span, we insure the consistency of each input series with ITRF/ICRF by removing the linear piecewise functions associated with networks instabilities. Then the formal uncertainties are multiplied by factor f related to the EOP and considered series.

Step 3: Differences of selected EOP series with respect to reference values.

We form the differences of the selected series to the smoothed C04—extended by a prediction (see step 6) and linearly interpolated to the epochs of the operational series—in order to mitigate uncertainty introduced by interpolation made further. However, this treatment is strictly applied to pole coordinates.

For UT1, it deserves some modifications. On one hand, we consider UT1-TAI instead of UT1-UTC to get rid of jumps associated with leap seconds that are inappropriate for numerical treatment of the series. On the other hand, UT1-TAI and LOD are corrected from the regular variations caused by zonal tides by removing the IERS model (Petit and Luzum 2010) in both selected and reference series before to compute the differences. This allows to mitigate interpolation error associated with the last procedure.

The removal of an a-priori model or time series is not necessary for nutation offsets to IAU 2000A and IAU 2006, for they are quantities smaller than 1 mas, and uncertainty brought by the interpolation method is then smaller than the nutation offset uncertainty. Note, however, that if celestial pole offsets were provided with respect to the IAU 1980 nutation–precession and/or were using $\Delta\psi$ and $\Delta\epsilon$ angles, they would be beforehand transformed into differences with respect to IAU 2000A/IAU 2006 in cartesian coordinates (Petit and Luzum 2010).

For a given EOP, the whole set of paired difference values is gathered, then chronologically sorted.

Step 4: Running average. The combination is based on a weighted average of the paired difference series over 0.5-day intervals for polar motion and UT1 and 1 day for nutation offsets. The observations p_j falling into each interval are propagated to the weighted mean date \bar{t} using cubic splines interpolation yielding \tilde{p}_j values, and their weighted average is formed according to

$$\bar{p} = \frac{\sum_{j=1}^n w_j \tilde{p}_j}{\sum_j w_j}, \quad (3)$$

where the data weights $w_j = 1/(f_j\sigma_j(t))^2$ are based on the calibrated formal uncertainties $f_j\sigma_j(\bar{t})$ introduced earlier. (There index j pertains to the series.)

Over a given year, the weighting of the series j for a given EOP is globally reflected by the calibrated mean uncertainty

$$\tilde{\sigma}_j^m = f_j\sigma_j^m. \quad (4)$$

As well as for the calibrating factor f_j , the time evolution of the yearly calibrated mean uncertainty is displayed in Fig. 3, giving also an overview of the combination itself year after year.

In one given interval, the selected values comes from IVS, IGS, ILRS combined series and their number n does not exceed 6. Eventually nutation and UT1 corrections are directly taken from the series of the IVS analysis centers, only for daily intervals where IVS-combined values are absent. In this respect, we assume that the uncertainties of the contributing values are independent, so that the standard error of the combined value can be computed by the formula

$$\bar{\sigma} = \frac{1}{\sqrt{\sum_{j=1}^n w_j}}. \quad (5)$$

Somehow the uncertainties associated with a given EOP series are reflected by their residuals with respect to the combined solution. We checked to which extent the time series constituted by these residuals are uncorrelated. For instance, according to Table 2, these correlations are below 0.2 over the period [2015.0–2018.0]. In the case of nutation correction dX , dY correlations with IVS-combined series are significant, but they are not pertinent in the sense that the contribution of USNO and BKG analysis centers only concerns the periods outside the $R1/R4$ session corresponding to IVS solution.

This step is completed by an outlier detection and rejection assuming a Gaussian distribution of the selected values around the C04 combined value \bar{p} : let wrms be the weighed root mean square of the distance of the selected values to the combined values, to find a selected values outside the window $[\bar{p} - 2.57 \text{ wrms}, \bar{p} + 2.57 \text{ wrms}]$ has a probability less than 1%, and such a value has its weight divided by 10. The combination step is looped back until convergence.

Step 5: Vondrak Smoothing, interpolation and adding back the intermediate series. The combined series is finally smoothed by a low-pass (Vondrák 1969) filter to remove spurious high-frequency variations introduced by the previous numerical procedures. The smoothing coefficient is chosen following the temporal resolution that can be reasonably reached with the corresponding technique/series (Table 3). The smoothed EOP values are then interpolated at 0 h UTC using Fourier (x , y) and cubic-spline interpolations (UT1, dX , dY). The final values of the C04 are obtained by adding back the guide signal previously removed, the zonal tides contributions to UT1-TAI and LOD, and translating UT1-TAI back to UT1-UTC.

Step 6: Storage in the database, extension by a prediction. For operational combination, the next solution needs reference

Table 2 Correlation coefficients between time series of the residuals of the contributing EOP solutions with respect to C04 solution over the period [2015.0–2018.0]

	IVS R x/y	ILRS x/y
IGS F x/y	0.09/0.13	− 0.19/− 0.09
IVS R x/y		− 0.12/− 0.04
	IAA intensive UT1	USNO intensive UT1
IVS UT1	0.09/0.13	0.07
IAA intensive UT1		0.12
	BKG dX/dY	GSFC dX/dY
IVS R dX/dY	0.63/0.54	0.69/0.52
BKG dX/dY		0.10/0.06

Table 3 Characteristics of the low-pass Vondrák filters used for the final smoothing of the 14C04 series: The 5% and 95% lines give the period (in days) for which the signal is attenuated by 95% and 5%, respectively

(%)	x , y	UT1	dX , dY	LOD
1984–1993				
5	1.2	1.2	3.3	1.2
95	3.2	3.2	8.8	3.2
1993–2000				
5	0.8	1.2	2.6	0.8
95	2.2	3.2	7.0	2.2
2000–2010				
5	0.6	0.8	2.6	0.6
95	1.5	2.2	7.0	1.5
2010–2015				
5	0.6	0.8	2.6	0.6
95	1.5	2.2	7.0	1.5

values covering the dates of the future observations. Therefore, we extend the present series by a prediction, based upon the extrapolation of a model composed of harmonic/linear terms, and of an autoregressive model of the residuals. In the case of pole coordinates, the harmonics are at 1-year, 0.5-year and 1.18-year (Chandler) periods. For UT1, the harmonics are restricted to the seasonal ones. The solution associated with its prediction is archived in our data base.

4 Operational treatment and dissemination

As new observations arrive at analysis centers, operational solutions are updated, so that last points can change between two solution runs. The C04 policy is considering that EOP values must be frozen if they are older than 30 days from the current epoch.

Table 4 Individual EOP series entering the C04 solution from 2015 onward

	x, y	UT1	dX, dY	LOD
ITRF 2014	<i>F</i>			<i>F</i>
VLBI IVS F (quarterly)	<i>F</i>	<i>F</i>	<i>F</i>	
VLBI IVS R (rapid)	<i>F/R</i>	<i>F/R</i>	<i>F/R</i>	
VLBI AUS		<i>R</i>	<i>R</i>	
VLBI BKG		<i>R</i>	<i>R</i>	
VLBI GSFC		<i>R</i>	<i>R</i>	
VLBI IAA		<i>R</i>	<i>R</i>	
VLBI OPA		<i>R</i>	<i>R</i>	
VLBI USNO		<i>R</i>	<i>R</i>	
VLBI GSFC intensive		<i>R</i>	<i>R</i>	
VLBI IAA intensive		<i>F/R</i>	<i>R</i>	
VLBI USNO intensive		<i>R</i>	<i>R</i>	
GNSS IGS final	<i>F/R</i>			<i>F/R</i>
GNSS IGS rapid	<i>R</i>			<i>R</i>
GNSS CODE	<i>R</i>			<i>R</i>
SLR ILRS	<i>F/R</i>			<i>F/R</i>
DORIS IDS	<i>F</i>			

The flag indicates whether the solution is used for the obtention of final (*F*) or rapid (*R*) values. These series can be downloaded from <http://iers.obspm.fr/eop-pc/index.php?index=analysis&lang=en/>

The 14C04 series run from 1962 to 30 days into the past. The whole series are recomputed every day taking into account the latest EOP determinations over one year into the past. These daily runs allow to refine preliminary values of the EOP for the last 30 days thanks to rapid solutions listed as R in Table 4. However, for several years, the older (final) EOP values are not refreshed between two ITRF updates, like ITRF 2008 and ITRF 2014. So, this rule discards the update of EOP solutions, like IVS quarterly combination solution, and thus mitigate quality of C04.

The IERS Bulletin B, published every month, publishes the last 14C04 month values (i.e., the penultimate month with respect to the ongoing one), which are considered as final values, as well as a preliminary extension running over the latest month. Official values for the last 30 days are given in the Bulletin A produced by IERS Rapid Service/Prediction Center (United States Naval Observatory). The 14C04 data and the IERS Bulletin B are available in ASCII format through the IERS EOC Internet server at <http://iers.obspm.fr/eop-pc>.

Rapid part of the pole coordinates being not covered by IGS final values (IGS F), we consider the IGS rapid values (IGS R) and complete them by CODE series (Bern University) in case of non-availability of IGS R data and for mitigating eventual errors.

UT1 intensive values are precious for determining not only the rapid or nearly real-time values but also final UT1 values. They have a larger uncertainty than the one derived from

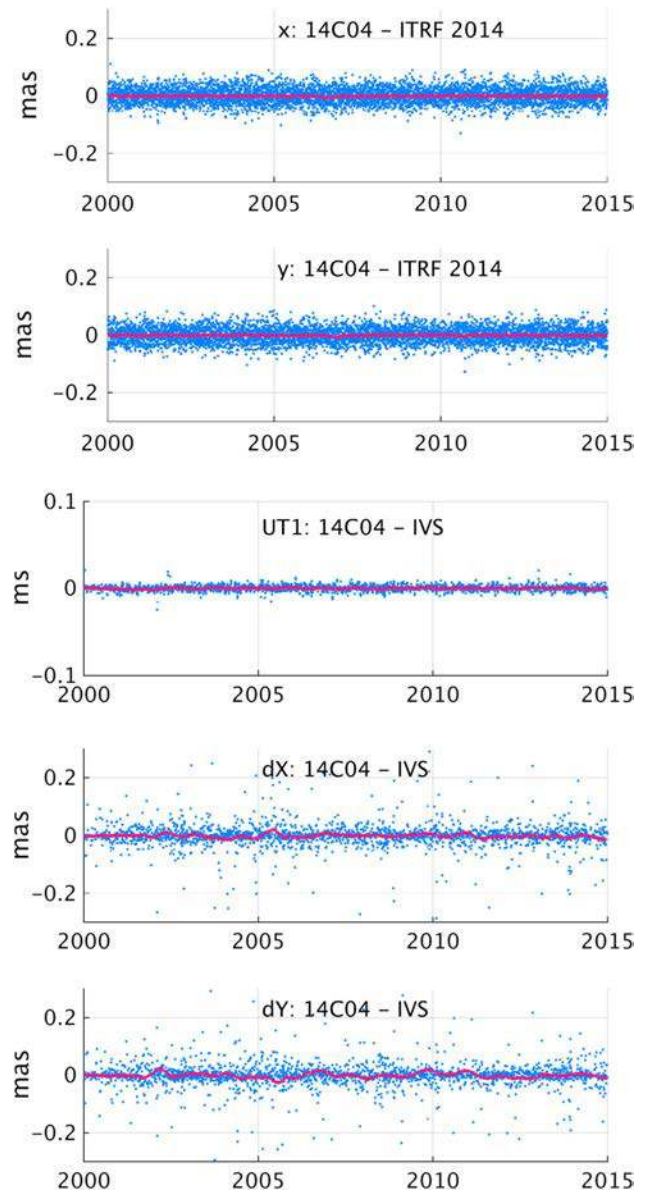


Fig. 4 Differences in (top) pole coordinates between 14C04 and ITRF 2014, and (bottom) UT1/nutation offsets between 14C04 and IVS. The thick, red curve represents a 3-month smoothing

$R1/R4$ VLBI session ($\sim 20 \mu\text{s}$ against $\sim 7 \mu\text{s}$). In this respect, intensive UT1 values are discarded when IVS values are available. Nonetheless, for the days with no $R1/R4$ sessions, UT1 is determined from the combination of intensive values (presently IAA intensive and USNO intensive). The pure interpolation between IVS values can introduce an interpolation error much larger than the uncertainty of intensive values.¹

¹ A test done on SLR satellite by Frank Reinquin (CNES) has shown that the C04 combination without intensive values causes large outliers in satellite orbit, personal communication.

Table 5 Averaged formal uncertainty of the 14C04 solution corresponding to four successive periods

	x	y	UT1	dX	dY	LOD
1984–1993	274	238	22.0	178	193	31
1993–2000	108	96	6.8	51	45	18
2000–2010	62	59	8.5	38	37	21
2010–2015	48	44	9.1	54	45	14

Unit is μas

5 Intra-technique consistency and accuracy

Figure 4 displays the differences between 14C04 and the ITRF 2014 pole coordinate series. No bias affects anymore the y -component as for the 08C04 series (Fig. 1). This is a direct effect of the modeling of mid-term excursions of the operational solutions with respect to the guide solutions with continuous piecewise linear functions. The standard deviation of the differences has been divided by a factor of two with respect to 08C04 (Table 5).

The 14C04 series better match the intra-technique combined solutions than the 08C04 version. This is evidenced by Table 6, where we report standard deviations of the differences between the C04 (both 08C04 and 14C04) and intra-technique and guide series. For pole coordinates, the

gain is about $10\mu\text{as}$ with respect to IGS solution from 2001 onward. For UT1, a gain of $3\mu\text{as}$ is noticeable after 2001 with respect to IVS solution. Nutation offsets evidence an improvement of about 30 to $60\mu\text{as}$ from 1993 onward.

We use the Allan standard deviation from 1993 to 2015 (see, e.g., for definition and applications of the Allan variance in geodesy Malkin 2016) to estimate the noise level and color of the differences between C04 and operational series of interest. Doing so, one can appreciate to which extent the C04 reproduces the operational series, and especially the guide series that are supposed to be the best representation of EOP in the conventional reference frames. In Fig. 5, we note that the Allan standard deviation is significantly smaller for the differences based on 14C04 than for 08C04, consistently with Table 6, except for LOD. (Indeed improvement in the C04 algorithm does not pertain to LOD.) For pole coordinates, the gain results from the fact that the input series of 14 C04 is the interpolated guide series. For nutation offsets, the better agreement with IVS series reflects the improvement brought in the combination procedure; the Allan deviation slope of ~ -0.5 indicates a white noise, in agreement with the fact that VLBI series differ from one another by white noise only (Bizouard 2018). For 08 C04 UT1, white noise stops after 200 days becoming a flicker noise. Meanwhile, for 14 C04 UT1 values, white noise feature continues till

Table 6 Standard deviation of the differences of C04 time series with IGS, IVS, and ILRS combined series and ITRF 2014

	08C04						14C04					
	x	y	UT1	dX	dY	LOD	x	y	UT1	dX	dY	LOD
1984–1993												
IGS F												
IVS F	121	110	7.4	90	89		344	291	12.0	100	104	
ILRS												
ITRF 2014	403	372	21.5				238	202	37.9			
1993–2001												
IGS F												
IVS F	103	95	9.4	67	60		70	55	4.4	34	37	
ILRS												
ITRF 2014	65	60	10.9				45	38	10.3			
2001–2010												
IGS F	49	37				13	41	33				18
IVS F	73	71	8.3	43	47		68	66	3.3	34	41	
ILRS	103	102				18	95	93				22
ITRF 2014	47	40	13.2				75	26	11.9			
2010–2015												
IGS F	42	36				11	31	27				10
IVS F	83	74	9.6	56	74		58	56	3.4	21	29	
ILRS	107	94				16	77	74				16
ITRF 2014	49	49	11.9				27	25	10.1			

Unit is μas

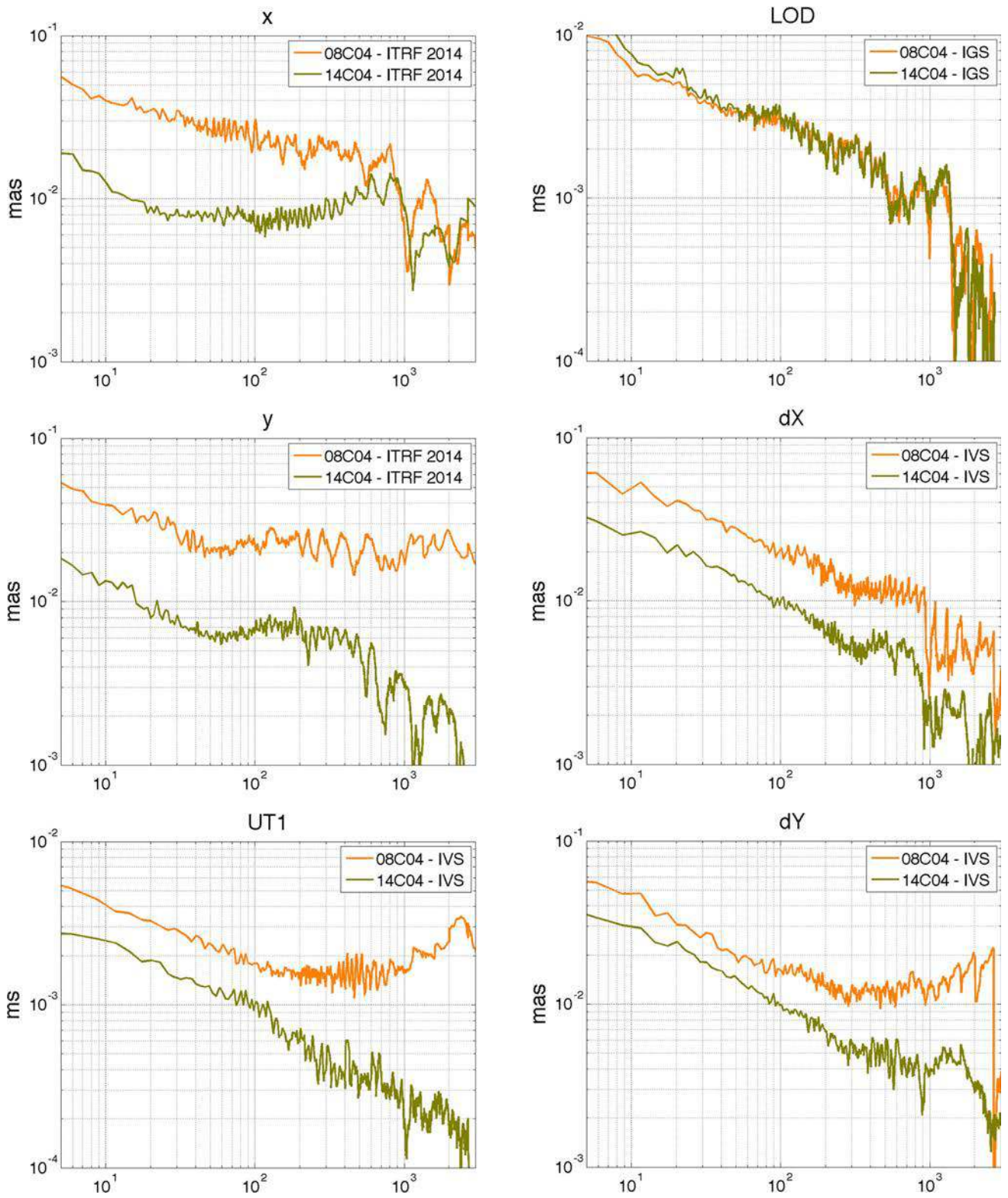


Fig. 5 Allan standard deviation of the differences of 08C04 (orange) and (green) 14C04 solutions with respect to three series (1993–2015). Differences are computed with respect to the ITRF 2014 series for pole

coordinates x and y, to IVS series for UT1 and nutation offsets, and IGS series for LOD

some thousand days. The meaning of the noise color is not clear but could be related to similar behaviors noticed in site coordinates estimated from the different techniques (Feissel-Vernier et al. 2007; Griffiths and Ray 2016). The fact that Allan standard deviation does not rise beyond 1000 days (in contrast to IGS data for x and y) ensures the long-term stabilities with respect to the guide series, and justify a posteriori the extrapolation of the “network effect” after the end of the guide series.

6 Conclusion

The IERS EOP 14C04 (abbreviated by 14C04) solution became the international reference EOP series on February 1, 2017, and replaced the IERS EOP 08C04. It is based on the combination of operational series as provided by the technique centers of IVS, IGS, ILRS, and IDS, as well as the EOP solution associated with the ITRF 2014 and operational solutions maintained by several IVS analysis centers and one IGS analysis center. The 14C04 has been strongly tied to two guide series, the IVS combination and the ITRF 2014 EOP solution, to ensure the consistency with the conventional reference frames ICRF2 (Fey et al. 2015) and ITRF 2014 (Altamimi et al. 2016). Other operational series were used to densify and extend the combined series after the ending of the guide series. Their impact is restricted to dates outside the $R1/R4$ VLI sessions for UT1, and it pertains to the rapid values or nearly real-time values, which are not given as IERS C04 product, but are derived for internal or national use. The Allan standard deviation of differences between the 14C04 and the guide series revealed a stability on time scales between 10 days and 3 years below $20\mu\text{s}$ for pole coordinates, $30\mu\text{s}$ for nutation offsets, and $3\mu\text{s}$ for UT1.

The realization of the C04 solution is also the opportunity for carrying out an extended statistic analysis of the EOP series produced by various analysis centers. Weighting of the selected intra-techniques solution is a way to grasp the evolution of techniques, as shown in Fig. 3.

Further evolutions of the 14C04 series will be undertaken after major releases of the conventional reference frames, and substantial improvements in the Earth’s rotation modeling (e.g., nutation model). We also plan to update more regularly final C04 values in order to account the release of quarterly IVS solution, and to correct possible erroneous values. As the radio-source CRF is more stable than TRF, the ITRF update has a larger impact on EOP estimates than generation of a new ICRF (Belda et al. 2017).

Acknowledgements The authors are grateful to N. Stamatakos and Z. Altamimi for their validation and analyses of the 14C04 solution; to D. Gambis, C. Hackman, J. Ray, Z. Malkin, E. Pavlis, and A. Nothnagel for their useful comments. This work was financially supported by CNES,

through the TOSCA program, and by the Scientific Council of the Paris Observatory.

References

- Abbondanza C, Chin TM, Gross RS, Heflin MB, Parker JW, Soja BS, van Dam T, Wu X (2017) JTRF2014, the JPL Kalman filter, smoother realization of the international terrestrial reference system. *J Geophys Res Solid Earth*. <https://doi.org/10.1002/2017JB014360>
- Altamimi Z, Collilieux X, Métivier L (2011) ITRF2008: an improved solution of the International Terrestrial Reference Frame. *J Geod* 8(85):457–473
- Altamimi Z, Rebischung P, Métivier L, Collilieux X (2016) A new release of the International Terrestrial Reference Frame modeling nonlinear station motions. *J Geophys Res Solid Earth* 8(121):6109–6131. <https://doi.org/10.1002/2016JB013098>
- Barnes RTH, Hide R, White AA, Wilson CA (1983) Atmospheric angular momentum fluctuations, length-of-day changes and polar motion. *Proc R Soc Lond Ser A* 387:31–73. <https://doi.org/10.1098/rspa.1983.0050>
- Bar-Sever Y, Russ KM (1997) New and improved solar radiation models for GPS satellites based on flight data. JPL Final Report (RF-182/808), 30 p
- Belda S, Heinkelmann R, Ferrándiz JM, Nilsson T, Schuh H (2017) On the consistency of the current conventional EOP series and the celestial and terrestrial reference frames. *J Geod* 91:135–149. <https://doi.org/10.1007/s00190-016-0944-3>
- Bizouard C (2018) Geophysical modelling of the polar motion. <http://www.degruyter.com/view/product/185549>
- Bizouard C, Gambis D (2009) The combined solution C04 for Earth orientation parameters consistent with International Terrestrial Reference Frame 2005. In: geodetic reference frames: IAG symposium Munich, Germany, 9–14 October 2006. Springer, Berlin, pp 265–270. <https://doi.org/10.1007/978-3-642-00860-341>
- Capitaine N, Wallace PT, Chapront J (2003) Expressions for IAU 2000 precession quantities. *Astron Astrophys* 2(412):567–586
- Chao BF (1984) Interannual length-of-day variation with relation to the Southern Oscillation/El Niño. *Geophys Res Lett* 5(11):541–544
- Chao BF, Hsieh Y (2015) The Earth’s free core nutation: formulation of dynamics and estimation of eigenperiod from the very-long-baseline interferometry data. *Earth Planet Sci Lett* 432:483–492
- Chao F, Yan H (2010) Relation between length-of-day variation and angular momentum of geophysical fluids. *J Geophys Res Solid Earth* B10:115. <https://doi.org/10.1029/2009JB007024>
- Chen JL, Wilson CR, Ries JC, Tapley BD (2013) Rapid ice melting drives Earth’s pole to the east. *Geophys Res Lett* 11(40):2625–2630. <https://doi.org/10.1002/grl.50552>
- Defraigne P, Smits I (1999) Length of day variations due to zonal tides for an inelastic Earth in non-hydrostatic equilibrium. *Geophys J Int* 2(139):563–572. <https://doi.org/10.1046/j.1365-246x.1999.00966.x>
- Dehant V, Feissel-Vernier M, de Viron O, Ma C, Yseboodt M, Bizouard C (2003) Remaining error sources in the nutation at the submilliarc second level. *J Geophys Res Solid Earth* B5:108. <https://doi.org/10.1029/2002JB001763>
- Dow JM, Neilan RE, Rizos C (2009) The international GNSS service in a changing landscape of global navigation satellite systems. *J Geod* 3(83):191–198. <https://doi.org/10.1007/s00190-008-0300-3>
- Durando G, Mana G (2002) Propagation of error analysis in least-squares procedures with second-order autoregressive measurement errors. *Meas Sci Technol* 10(13):1505

- Feissel-Vernier M, de Viron O, Le Bail K (2007) Stability of VLBI, SLR, DORIS, and GPS positioning. *Earth Planets Space* 59:475–497
- Fey AL, Gordon D, Jacobs CS, Ma C, Gaume RA, Arias EF, Bianco G, Boboltz DA, Böckmann S, Bolotin S et al (2015) The second realization of the international celestial reference frame by very long baseline interferometry. *Astron J* 2(150):58
- Gipson J (2007) Incorporating correlated station dependent noise improves VLBI estimates. In: *Proceeding of the 18th European VLBI for geodesy and astrometry working meeting*, Vienna, pp 12–13
- Griffiths J, Ray J (2016) Impacts of GNSS position offsets on global frame stability. *Geophys J Int* 1(204):480–487. <https://doi.org/10.1093/gji/ggv455>
- Herring TA, Mathews PM, Buffett BA (2002) Modeling of nutation–precession: very long baseline interferometry results. *J Geophys Res Solid Earth* B4:107. <https://doi.org/10.1029/2001JB000165>
- Hide R, Boggs Dale H, Dickey JO (2000) Angular momentum fluctuations within the Earth’s liquid core and torsional oscillations of the core–mantle system. *Geophys J Int* 3(143):777–786
- Holme R, de Viron O (2013) Characterization and implications of intradecadal variations in length of day. *Nature* 7457(499):202–204
- IDS, International DORIS Service (2018). <https://ids-doris.org>
- Kalarus M, Schuh H, Kosek W, Akyilmaz O, Bizouard C, Gambis D, Gross R, Jovanović B, Kumakshev S, Kutterer H, Mendes Cerveira PJ, Pasynok S, Zotov L (2010) Achievements of the Earth orientation parameters prediction comparison campaign. *J Geod* 84:587–596. <https://doi.org/10.1007/s00190-010-0387-1>
- Malkin Z (2016) Application of the allan variance to time series analysis in astrometry and geodesy: a review. *IEEE Trans Ultrason Ferroelectr Freq Control* 4(63):582–589. <https://doi.org/10.1109/TUFFC.2015.2496337>
- Mathews PM, Herring TA, Buffett BA (2002) Modeling of nutation and precession: new nutation series for nonrigid Earth and insights into the Earth’s interior. *J Geophys Res Solid Earth* B4:107. <https://doi.org/10.1029/2001JB000390>
- Pearlman M, Noll C, Dunn P, Horvath J, Husson V, Stevens P, Torrence M, Vo H, Wetzel S (2005) The international laser ranging service and its support for IGGOS, the global geodetic observing system. *J Geodyn* 4–5(40):470–478. <https://doi.org/10.1016/j.jog.2005.06.009>
- Petit G, Luzum B (2010) IERS conventions 2010. IERS Technical Note 36. Verlag des Bundesamts für Kartographie und Geodäsie, Frankfurt am Main, p 179
- Plag H-P, Beutler G, Gross R, Herring TA, Poli P, Rizos C, Rothacher M, Rummel R, Sahagian D, Zumberge J (2009) Recommendations. In: Plag H-P, Michael P (eds) *Global geodetic observing system: meeting the requirements of a global society on a changing planet in 2020*, pp 283–291. https://doi.org/10.1007/978-3-642-2687-4_11
- Ponte RM, Stammer D, Marshall J (1998) Oceanic signals in observed motions of the Earth’s pole of rotation. *Nature* 6666(391):476–479. <https://doi.org/10.1038/35126>
- Ray RD, Erofeeva SY (2014) Long-period tidal variations in the length of day. *J Geophys Res Solid Earth* 2(119):1498–1509. <https://doi.org/10.1002/2013JB010830>
- Rosen Richard D, Salstein David A (1983) Variations in atmospheric angular momentum on global and regional scales and the length of day. *J Geophys Res Oceans* C9(88):5451–5470. <https://doi.org/10.1029/JC088iC09p05451>
- Seitz M, Blossfeld M, Angermann D, Schmid R, Gerstl M, Seitz F (2016) The new DGFI-TUM realization of the ITRS: DTRF2014 (data). PANGAEA. <https://doi.org/10.1594/PANGAEA.864046>
- Schuh H, Behrend D (2012) VLBI: a fascinating technique for geodesy and astrometry. *J Geodyn* 61:68–80
- Vondrák J (1969) A contribution to the problem of smoothing observational data. *Bull Astron Inst Czechoslov* 349:20
- Willis P, Fagard H, Ferrage P, Lemoine FG, Noll CE, Noomen R, Otten M, Ries JC, Rothacher M, Soudarin L, Tavernier G, Valette J-J (2010) The international DORIS service (IDS): toward maturity, DORIS: scientific applications in geodesy and geodynamics. *Adv Space Res* 12(45):1408–1420. <https://doi.org/10.1016/j.asr.2009.11.018>
- Yoder CF, Williams JG, Dickey JO, Schutz BE, Eanes RJ, Tapley BD (1983) Secular variation of Earth’s gravitational harmonic J2 coefficient from LAGEOS and nontidal acceleration of Earth rotation. *Nature* 303:757–762. <https://doi.org/10.1038/303757a0>
- Zhu SY, Mueller II (1983) Effects of adopting new precession, nutation and equinox corrections on the terrestrial reference frame. *Bull Géod* 1(57):29–42. <https://doi.org/10.1007/BF02520910>